The Point Spread Function and Optical Dot Gain

Geoffrey L. Rogers
Fashion Institute of Technology, New York, NY, USA

1 Introduction

Optical dot gain, which is also known as the Yule–Nielsen effect [1–3], has a significant effect on halftone tonality and is caused by the diffusion of photons within the paper upon which the halftone is printed. Any physical model of halftone reflectance must take this effect into consideration in order to accurately predict halftone color.

Because of photon diffusion within the paper, a photon may exit the paper from a point different from that which it entered the paper. A photon may enter the paper in a region that is void of ink and exit the paper in a region that is covered by ink so that the absorption of light is greater than one would expect based only on dot size. There is an effective dot size that is larger than the actual dot size. This is illustrated in Figure 1.

In this article, optical dot gain is modeled using a point spread function (PSF) [4] and a PSF is obtained by physically modeling the interaction of light with paper. In Section 1, the concept of PSF is explained. In Section 2, a model for halftone reflectance, which includes optical dot gain, is developed using a PSF. It is shown that the Yule–Nielsen n value [1, 2] lies between 1 and 2 for the case treated here (nonscattering ink, no ink penetration into the paper, and no multiple internal reflections). In Section 3, the photon distribution within the paper is calculated by solving the radiative transfer equation in the diffusion approximation. On the basis of the light flux within the paper, a diffusion PSF is obtained in Section 4. Section 5 shows the connection between the PSF approach and the probability approach to optical dot gain. The probability approach uses the probabilities of diffusion between different regions of the halftone microstructure to account for optical dot gain. It is shown that the expressions for the halftone reflectance is identical in the two approaches and that the probabilities can be calculated from the PSF.

Handbook of Digital Imaging, Online © 2015 John Wiley & Sons, Ltd.

This article was published in the *Handbook of Digital Imaging* in 2015 by John Wiley & Sons, Ltd.
DOI: 10.1002/9781118798706.hdi052

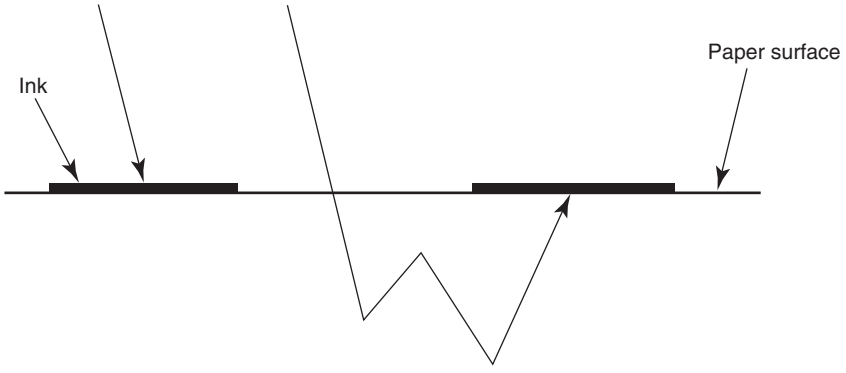

Figure 1 Optical dot gain: photons that are incident between the dots can still be absorbed by the ink due to diffusion

1.1 Point Spread Function

The concept of a PSF arises from the input–output relationships for linear systems [4]. Let $f(x, y)$ represent the input and $g(x, y)$ the output of a linear system. If the system is represented by the operator $\mathcal{S}\{\ \}$, then

$$g(x, y) = \mathcal{S}\{f(x, y).$$

One can write $f(x, y)$ as

$$f(x, y) = \int\int_{\infty}^{\infty} f(x', y')\delta(x - x')\delta(y - y')\mathrm{d}x'\mathrm{d}y'$$

and the output is

$$g(x, y) = \mathcal{S}\left\{\int\int_{\infty}^{\infty} f(x', y')\delta(x - x')\delta(y - y')\mathrm{d}x'\mathrm{d}y'\right\}.$$

Owing to the linearity of the system, this can be written as

$$g(x, y) = \int\int_{\infty}^{\infty} f(x', y')\mathcal{S}\{\delta(x - x')\delta(y - y')\mathrm{d}x'\mathrm{d}y'\}.$$

The response of the system to an impulse input:

$$H(x, x'; y, y') = \mathcal{S}\{\delta(x - x')\delta(y - y')\}$$

is the PSF. It is the two-dimensional analog of the impulse response in electronic circuits. If the linear system is stationary, which is assumed here, then the PSF can be written as $H(x - x', y - y')$.

Historically, PSFs have been used to characterize the resolving capabilities of optical systems such as a telescope. Owing to diffraction effects and aberrations in optical systems, the image of a point source of light, such as a star, is blurred or distorted. A PSF characterizes

DOI: 10.1002/9781118798706.hdi052

the distortion. PSFs have also been used to characterize the resolution of imaging media or capture devices such as film or charge-coupled device (CCD) arrays [4–7].

As used in quantifying the optics of the paper, however, one is not interested in using the PSF to characterize the resolution. The highest spatial frequencies resolved in a halftone image are much less than the halftone screen frequency, r^{-1}. Here, the PSF is used to characterize the diffusion of light within the paper and the average diffusion length (the average distance a photon diffuses within the paper) is generally comparable in size to the screen period r. The normalized PSF $H(x - x', y - y')$ is essentially the probability density that a photon entering the paper at point (x', y') will exit the paper at point (x, y). The PSFs considered here are assumed to be radially symmetric: $H(x, y) = H(\rho)$, where $\rho = \sqrt{x^2 + y^2}$ is the radial distance.

Closely related to the PSF is the line spread function (LSF) [3, 4, 8], which is the response to a line impulse. It is related to the PSF as

$$L(x) = \int_{-\infty}^{\infty} H(x, y)\, \mathrm{d}y.$$

Also related to the PSF and LSF is the edge spread function (ESF) [4]:

$$E(x) = \int_{-\infty}^{x} L(x')\, \mathrm{d}x' \tag{1}$$

which is the response to a knife edge. From Equation 1, one sees that

$$L(x) = \frac{\mathrm{d}E(x)}{\mathrm{d}x}. \tag{2}$$

Figure 2 shows a typical PSF, LSF, and ESF. Another important quantity is the modulation transfer function (MTF). The MTF characterizes the frequency response of the paper and is a zero-order Hankel transform of the PSF and a Fourier transform of the LSF.

A PSF was first used to quantify the photon diffusion in halftone paper by Yule *et al.* [9] in 1967. They measured the PSF width (having assumed a Gaussian PSF) using the edge gradient method [8, 10]. Measuring several types of paper, they found that there was a good correlation between the effective dot area minus actual dot area and the PSF width. Measurements of the PSF by Wakeshima *et al.* [11] in 1968 suggested an exponential shape. They illuminated the paper at a single point with a thin pencil of light, and measured the reflected flux as a function of distance from the point of entry. In 1978, Ruckdeschel and Hauser used a Gaussian PSF to

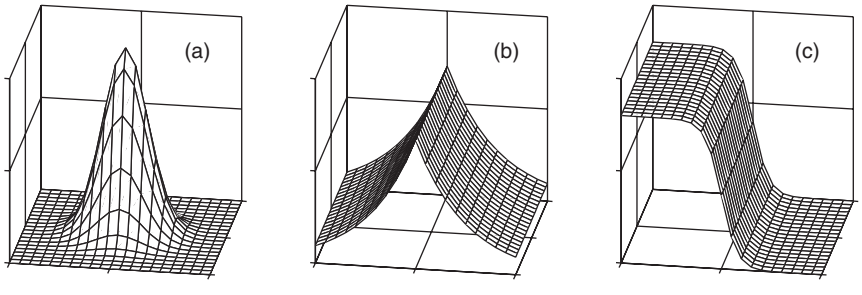

Figure 2 A typical (a) PSF, (b) LSF, and (c) ESF

Handbook of Digital Imaging, Online © 2015 John Wiley & Sons, Ltd.

This article was published in the *Handbook of Digital Imaging* in 2015 by John Wiley & Sons, Ltd.
DOI: 10.1002/9781118798706.hdi052

derive an expression for the Yule–Neilson n-factor [12]. In 1982, Oittinen [13] conjectured a theoretical PSF based on Kubelka–Munk theory. In 1995, Engeldrum and Pridham measured the MTF using the edge gradient method for several types of paper and compared it to the MTF derived from Oittinen's theoretical PSF. They found that the Kubelka–Munk-based MTF and the measured MTF had poor agreement for coated papers and good agreement for newsprint and typewriter bond at low frequencies. In the late 1990s and early 2000s, Arney with a number of different workers made a number of measurements of paper MTF and compared it with both phenomenological and Kubelka–Munk-derived theoretical MTFs [14–16]. In 1997, Rogers [3] derived a theoretical PSF using the diffusion approximation to the radiative transfer equation. That derivation is given in Sections 4 and 5 of this article. Yang [17–20] has done extensive theoretical work extending the Kubelka–Munk theory to account for optical dot gain. Mourad [21, 22] obtained an MTF of paper using an extended Kubelka–Munk theory.

2 Halftone Reflectance

In the following, one obtains an expression for the halftone reflectance (the average reflectance) from a region of a halftone print in terms of the halftone microstructure – the ink transmission and size and shape of the dots – and the effects of the paper. The ink is laid on the paper in the form of circular dots with radius d, and dot centers fall on a square lattice (screen grid) with screen period r, that is, the distance between neighboring dots is r. One considers a region of the halftone that has a constant tone, that is, the size of the dots is constant over the region and the region is large compared to the screen period.

The bare paper has reflectance R_p, and the ink forms a thin layer that lies on top of the paper surface. The inks are purely absorbing (no scatter) and the ink does not penetrate into the paper [23]. Internal reflection at the paper–air boundary is not taken into consideration [24]. The light is natural –incoherent, unpolarized white light –and diffuse. In expressions involving radiation, wavelength dependence is suppressed for notational simplicity. It is assumed that paper material properties are wavelength independent; ink may have wavelength dependence, but again, for notational simplicity wavelength dependence is suppressed.

The average reflectance is found by averaging the point reflectance over the region:

$$\bar{R} = \frac{1}{(Nr)^2} \int R(x, y) \mathrm{d}A \tag{3}$$

where $\mathrm{d}A = \mathrm{d}x\,\mathrm{d}y$ is an element of area, N^2 the number of dots in the region, and $(Nr)^2$ the area of the region. The region consists of N^2 cells of area r^2, and each cell contains one dot. For simplicity in all that follows, one takes the limit $N \to \infty$.

The point reflectance is the reflectance at point (x, y) and is given by Ruckdeschel and Hause [12]:

$$R(x, y) = R_\mathrm{p} T(x, y) \int \int T(x', y') H(x - x', y - y') \mathrm{d}x' \mathrm{d}y'. \tag{4}$$

The quantity $H(x - x', y - y')$ is the paper's PSF, so that $R_\mathrm{p} H(x - x', y - y')$ is the probability that a photon entering the paper at point (x', y') exits the paper at point (x, y). As the reflectance of the bare paper is R_p, $H(x, y)$ is normalized to unity. The transmission function $T(x, y)$ is the

Handbook of Digital Imaging, Online © 2015 John Wiley & Sons, Ltd.

This article was published in the *Handbook of Digital Imaging* in 2015 by John Wiley & Sons, Ltd.
DOI: 10.1002/9781118798706.hdi052

transmittance of the ink layer at the point (x, y). Those areas of the paper between the dots (no ink) have transmittance of 1. The areas covered by ink have transmittance T_0, where wavelength dependence has been suppressed to ease the notation. One can express the transmission function as

$$T(x, y) = 1 - C(x, y) + T_0 C(x, y) = 1 - (1 - T_0)C(x, y) \tag{5}$$

where the characteristic function $C(x, y)$ is 1 if there is ink at point (x, y) and 0 if there is no ink at that point. This function is a convolution of the dot distribution function, and a function that describes the shape of the dots:

$$C(x, y) = \text{circ}\left[\frac{\sqrt{x^2 + y^2}}{d}\right] * g \tag{6}$$

where d is the radius of the (circular) dots, $*$ indicates a convolution, and the distribution function for the dots is

$$g(x, y) = \sum_{n,m} \delta(x - nr)\delta(y - mr) \tag{7}$$

where $\delta(x)$ is the Dirac delta function. The shape function for circular dots, circ$[u]$, is defined by

$$\text{circ}[u] = \begin{cases} 1 & u \leq 1 \\ 0 & u > 1 \end{cases}. \tag{8}$$

Carrying out the convolution, one obtains

$$C(x, y) = \sum_{n,m} \text{circ}\left[\frac{\sqrt{(x - nr)^2 + (y - mr)^2}}{d}\right]. \tag{9}$$

Expanding Equation 4 using Equation 5, one obtains for the point reflectance:

$$R(x, y) = [1 - (1 - T_0)C(x, y) - (1 - T_0)P(x, y) + (1 - T_0)^2 C(x, y)P(x, y)]R_\text{p} \tag{10}$$

where $P(x, y)$ is defined as

$$P(x, y) = \int\int C(x', y')H(x - x', y - y')\text{d}x'\text{d}y'. \tag{11}$$

The quantity $P(x, y)$ is a double convolution and can be evaluated by taking the inverse Fourier transform of the product of the Fourier transforms of the convolution operands. The Fourier transform of $P(x, y)$ is

$$\mathcal{F}\{P(x, y)\} = \mathcal{F}\{\text{circ}[\rho/d]\}\mathcal{F}\{g(x, y)\}\mathcal{F}\{H(x, y)\}, \tag{12}$$

where $\mathcal{F}\{\}$ indicates a Fourier transform. The Fourier transform of circ$[\rho/d]$ is readily obtained:

$$\mathcal{F}\{\text{circ}[\rho/d]\} = d^2 \frac{J_1(2\pi\omega d)}{\omega d} \tag{13}$$

Handbook of Digital Imaging, Online © 2015 John Wiley & Sons, Ltd.

This article was published in the *Handbook of Digital Imaging* in 2015 by John Wiley & Sons, Ltd.
DOI: 10.1002/9781118798706.hdi052

where $J_1(x)$ is the first-order Bessel function, and ω is the magnitude of the two dimensional spatial frequency (in cycles/unit length).

The Fourier transform of the dot distribution is also readily obtained:

$$\mathcal{F}\{g(x,y)\} = \frac{1}{r^2}\sum_{n,m}\delta(\omega_x - n/r)\delta(\omega_y - m/r), \tag{14}$$

where ω_x and ω_y are x and y components of the spatial frequency.

The Fourier transform of $H(x,y)$ is the optical transfer function (OTF) of the paper [4]. Because of the assumed symmetry and reality of $H(x,y)$, the OTF is identical to the paper's MTF and is radially symmetric in frequency space:

$$\tilde{H}(\omega) = \mathcal{F}\{H(x,y)\}, \tag{15}$$

where $\tilde{H}(\omega)$ is the MTF of the paper.

Taking the inverse Fourier transform of Equation 12, one obtains for $P(x,y)$:

$$P(x,y) = \frac{\pi d^2}{r^2}\sum_{n,m}\mathcal{J}_{nm}\tilde{H}_{nm}\exp\,[-2\pi i(nx+my)/r], \tag{16}$$

where one defines

$$\mathcal{J}_{nm} = \frac{J_1(2\pi\sqrt{n^2+m^2}d/r)}{\pi\sqrt{n^2+m^2}d/r} \tag{17}$$

and

$$\tilde{H}_{nm} = \tilde{H}\left((\sqrt{n^2+m^2}/r\right). \tag{18}$$

Note that $\mathcal{J}_{00} = \tilde{H}_{00} = 1$.

One obtains the halftone or average reflectance from the region by averaging the point reflectance $R(x,y)$ over all x,y. Using Equation 10 in Equation 3, there are four terms to integrate. The first term is clearly equal to 1. The second term is

$$(1-T_0)\frac{1}{(Nr)^2}\iint \mathrm{circ}\left[\frac{\sqrt{x^2+y^2}}{d}\right] * g\,\mathrm{d}x\mathrm{d}y \tag{19}$$

which evaluates to $(1-T_0)\pi(d/r)^2$.

The third term is

$$(1-T_0)\frac{1}{(Nr)^2}\iint P(x,y)\,\mathrm{d}x\mathrm{d}y \tag{20}$$

which also evaluates to $(1-T_0)\pi(d/r)^2$.

The fourth term is

$$(1-T_0)^2\frac{1}{(Nr)^2}\iint \mathrm{circ}\left[\frac{\sqrt{x^2+y^2}}{d}\right] * gP(x,y)\mathrm{d}x\mathrm{d}y \tag{21}$$

Handbook of Digital Imaging, Online © 2015 John Wiley & Sons, Ltd.
This article is © 2015 John Wiley & Sons, Ltd.
This article was published in the *Handbook of Digital Imaging* in 2015 by John Wiley & Sons, Ltd.
DOI: 10.1002/9781118798706.hdi052

which can be written as

$$\frac{\pi(d/r)^2}{(Nr)^2}\sum_{nmn'm'}\mathcal{J}_{nm}\tilde{H}_{nm} \times\iint \text{circ}\left[\sqrt{(x-n'r)^2+(y-m'r)^2}/d\right]\exp[-2\pi i(nx+my)/r]\mathrm{d}x\,\mathrm{d}y \quad (22)$$

Substituting $u = x - n'r$ and $v = y - m'r$, the double integral can be written as

$$\exp[-2\pi i(nn'+mm')]\iint \text{circ}\left[\frac{\sqrt{u^2+v^2}}{d}\right]\exp\ [2\pi i(nu+mv)/r]\mathrm{d}u\mathrm{d}v. \quad (23)$$

The first exponential is equal to 1 for all n, m, n', m' and the double integral is identically $\pi d^2\mathcal{J}^*_{nm}$ so the fourth term becomes

$$\pi^2(d/r)^4(1-T_0)^2\sum_{nm}|\mathcal{J}_{nm}|^2\tilde{H}_{nm}. \quad (24)$$

Thus, one can write the average reflectance from the region as

$$\bar{R} = R_\mathrm{p}[1-2\mu(1-T_0)+\mu^2(1-T_0)^2\mathcal{Z}], \quad (25)$$

where $\mu = \pi(d/r)^2$ is the fractional area covered by the dots, and

$$\mathcal{Z} = \sum_{nm}|\mathcal{J}_{nm}|^2\tilde{H}_{nm} \quad (26)$$

The summation $\mathcal{Z}$ completely contains the effects of the optical dot gain. It is a function of dot shape, dot size, screen period, and the photon diffusion characteristics of the paper. It is shown later that $\mu\mathcal{Z}$ is the probability that a photon exits the paper through a dot if it originally entered through a dot and that one can interpret $\mathcal{Z}^{-1}$ as an effective diffusion area.

The quantity $\mathcal{Z}$ can be written as a somewhat simpler expression. Defining p_k as the number of points in a square lattice on a circle of radius $\sqrt{k}$ [25], one can write

$$\mathcal{Z} = \sum_{k=0}^{\infty}p_k|\mathcal{J}_k|^2\tilde{H}_k \quad (27)$$

with

$$\mathcal{J}_k = \frac{J_1\left(2\sqrt{\pi k\mu}\right)}{\sqrt{\pi k\mu}} \quad (28)$$

and

$$\tilde{H}_k = \tilde{H}\left(\sqrt{k}/r\right). \quad (29)$$

Although the expression for $\bar{R}$ has been derived for circular dots, the average reflectance has the same form as Equation 25 for dots of any shape, with $\mathcal{Z}$ given by Equation 26 and the definition of $\mathcal{J}_{nm}$ generalized. If the dots have a shape function given by $w(x, y)$ ($w(x, y) = 1$ if

Handbook of Digital Imaging, Online © 2015 John Wiley & Sons, Ltd.

This article was published in the *Handbook of Digital Imaging* in 2015 by John Wiley & Sons, Ltd.
DOI: 10.1002/9781118798706.hdi052

the point (x, y) lies inside the dot and 0 otherwise) and lie on a lattice with period r, then one can define $\mathcal{J}_{nm}$ as

$$\mathcal{J}_{nm} = \frac{\iint w(x,y) \exp\ [2\pi i(nx + my)/r]\mathrm{d}x\,\mathrm{d}y}{\iint w(x,y)\mathrm{d}x\mathrm{d}y} \tag{30}$$

For example, if the dots are square with sides of length d, then $w(x, y) = \mathrm{rect}(x/d)\mathrm{rect}(y/d)$, where $\mathrm{rect}(u) = 1$ if $|u| \leq 1$ and 0 otherwise, one finds that

$$\mathcal{J}_{nm} = \mathrm{sinc}(nd/r)\mathrm{sinc}(md/r) \tag{31}$$

with $\mathrm{sinc}(v) = \sin(\pi v)/(\pi v)$.

To give the expression for $\bar{R}$ a physical meaning, one considers two extreme cases: the average distance a photon diffuses is (i) much larger than the screen period (complete diffusion) and (ii) much smaller than a screen period (no diffusion). It is shown that the two extremes correspond to the Yule–Nielsen n factor equalling 2 and 1, respectively. (For simplicity, in the following, one sets $R_\mathrm{p} = 1$.) The average distance a photon diffuses, the diffusion length, is the first moment of the PSF:

$$\bar{\rho} = 2\pi \int \rho H(\rho) d\rho. \tag{32}$$

The approximate bandwidth of the paper is $1/\bar{\rho}$.

If $\bar{\rho}$ is much larger than the screen period, $\bar{\rho}/r \gg 1$, then $\tilde{H}(k) \approx 0$ for $k \geq 1/r$. Therefore, $\tilde{H}_{nm} \approx 0$ for $n, m \neq 0$ so that

$$\mathcal{Z} = 1. \tag{33}$$

The average reflectance in this case is

$$\bar{R} = 1 - 2\mu(1 - T_0) + \mu^2(1 - T_0)^2 = [1 - \mu(1 - T_0)]^2 \tag{34}$$

The reflectance of the ink is $R_i = T_0^2$ (the paper reflectance is taken to be 1), so the average reflectance can be written as

$$\bar{R} = [1 - \mu(1 - R_i^{1/2})]^2, \tag{35}$$

which is the Yule–Nielsen equation [1] with $n = 2$.

If the diffusion length is very small compared to the screen period, $\langle\rho\rangle/r \to 0$, then $\tilde{H}(k) \approx 1$ for all $k < 1/\langle\rho\rangle \to \infty$. The $\tilde{H}_{nm} \approx 1$ for all relevant n, m and

$$\mathcal{Z} = \sum_{n,m} |\mathcal{J}_{nm}|^2. \tag{36}$$

This sum can be evaluated exactly using the definition of $\mathcal{J}_{nm}$, Equation 30. One can write

$$\sum_{n,m} |\mathcal{J}_{nm}|^2 = A^{-2} \iiiint w(x,y)w^*(x',y') \sum_n \exp\ [2\pi in(x - x')/r] \times \sum_m \exp\ [2\pi im(y - y')/r]\mathrm{d}x\,\mathrm{d}x'\,\mathrm{d}y\,\mathrm{d}y'. \tag{37}$$

Handbook of Digital Imaging, Online © 2015 John Wiley & Sons, Ltd.

This article was published in the *Handbook of Digital Imaging* in 2015 by John Wiley & Sons, Ltd.
DOI: 10.1002/9781118798706.hdi052

where $A = \iint w(x, y)\mathrm{d}x\,\mathrm{d}y =$ the area of the dot. Noting that

$$\sum_n \exp\ [2\pi in(x - x')/r] = r\delta(x - x'), \tag{38}$$

and $|w(x, y)|^2 = w(x, y)$, one finds

$$\mathcal{Z} \approx \mu^{-1} \tag{39}$$

where μ is the fractional arc covered by a dot, that is, the ratio of dot area to cell area r^2. The average reflectance in this case is

$$\bar{R} = 1 - \mu(1 - R_i). \tag{40}$$

This is the Murray–Davis equation [26, 27], the average reflectance when there is no photon diffusion within the paper, which is also the Yule–Nielsen equation with $n = 1$. In this case, there is no optical dot gain.

As explicitly shown here, the extremes of no diffusion and complete diffusion correspond to a Yule–Nielsen n values of 1 and 2, as has been suggested by a number of authors [2, 12, 26]. A model in which multiple internal reflections are included, however, can result in n values significantly greater than 2 [24].

3 Radiative Transfer

In this section, a distribution function for photons within the paper is obtained by solving the radiative transport equation [28, 29] using the diffusion approximation [3, 30–35]. The photon distribution is then used to construct a PSF.

In the model constructed here, an infinitely thin stream of photons is incident normally on the paper surface and these injected photons scatter and become nearly diffuse. The distribution of these nearly diffuse photons is calculated, and the PSF is the normalized outward flux of these diffuse photons as a function of the distance from the point of incidence.

Paper consists of a very complex network of layers of flattened cellulose fibers plus filler pigments such as titanium dioxide or calcium carbonate [36]. The transparent flattened fibers have ∼75 μm width and ∼ 8 μm thickness [37] and an index of refraction of [38] $n \approx 1.5$. The thickness of the paper is typically 10 to 18 fiber layers [37]. The degree of absorption within white paper is quite small –the paper opacity is due to scattering. The model used here treats paper in a simplified way. The model ignores fiber orientation [37] and the multilayer structure [39], and assumes that the paper is isotropic and homogeneous. The paper is characterized by its thickness, t, by two physical properties of the paper, the scattering coefficient, γ_s, and the absorption coefficient, γ_a, and by an anisotropic scattering parameter, g.

Because of the symmetry, polar coordinates (z, ρ, ϕ) are used with the z axis perpendicular to the paper surface, and $+z$ pointing into the paper (pointing downward) and $z = 0$ at the paper surface. The paper has thickness t, so the bottom surface of the paper is at $z = t$. Photons are incident on the paper at a single point: $z = 0$ and $\rho = 0$ and are traveling in the $+z$ direction. Photons are treated as billiard balls undergoing elastic collisions with stationary scatterers traveling at speed c between collisions. As in Section 2, one assumes natural light – incoherent, unpolarized white light. In expressions involving radiation, wavelength dependence is suppressed for notational simplicity. It is assumed that paper material properties are wavelength independent. Any interference effects are assumed to average to zero.

Handbook of Digital Imaging, Online © 2015 John Wiley & Sons, Ltd.

This article was published in the *Handbook of Digital Imaging* in 2015 by John Wiley & Sons, Ltd.
DOI: 10.1002/9781118798706.hdi052

3.1 Diffusion Equation

A stream of photons is incident on the paper at the origin. The scattering of these injected photons is the source of nearly diffuse photons. The steady-state radiative transfer equation for the photon distribution is [28, 29]

$$\hat{\mathbf{s}} \cdot \nabla f(\mathbf{r}, \hat{\mathbf{s}}) = -\gamma_t f(\mathbf{r}, \hat{\mathbf{s}}) + \frac{\gamma_s}{4\pi} \int_{(4\pi)} p(\hat{\mathbf{s}}, \hat{\mathbf{s}}') f(\mathbf{r}, \hat{\mathbf{s}}) \, \mathrm{d}\Omega' \tag{41}$$

where $f(\mathbf{r}, \hat{\mathbf{s}})$, the photon distribution, is the number of photons per unit volume per unit solid angle at position $\mathbf{r}$ traveling in direction $\hat{\mathbf{s}}$. This is related to the radiance $I(\mathbf{r}, \hat{\mathbf{s}})$ (power per unit area per unit solid angle) as $I(\mathbf{r}, \hat{\mathbf{s}}) = c\varepsilon f(\mathbf{r}, \hat{\mathbf{s}})$ with ε the photon energy. The extinction coefficient is the sum of the scattering and absorption coefficients: $\gamma_t = \gamma_s + \gamma_a$. The phase function $p(\hat{\mathbf{s}}, \hat{\mathbf{s}}')$ is the normalized differential scattering cross section and is the probability per unit solid angle that a photon originally traveling in the direction $\hat{\mathbf{s}}'$ is traveling in the direction $\hat{\mathbf{s}}$ after scattering. The phase function is normalized such that $(4\pi)^{-1} \int p(\hat{\mathbf{s}}, \hat{\mathbf{s}}') \mathrm{d}\Omega' = 1$ and depends only on the angle between $\hat{\mathbf{s}}$ and $\hat{\mathbf{s}}'$. A commonly used phenomenological phase function is

$$p(\hat{\mathbf{s}}, \hat{\mathbf{s}}') = (1 - g) + 4\pi g \delta(\hat{\mathbf{s}} \cdot \hat{\mathbf{s}}'). \tag{42}$$

The first term represents the isotropic scattering and the second term represents the forward or backward scattering, depending on the value of g: $-1 \leq g \leq 1$, where g is the average cosine of the scattering angle: $g = \langle \hat{\mathbf{s}} \cdot \hat{\mathbf{s}}' \rangle = \int p(\hat{\mathbf{s}}, \hat{\mathbf{s}}') \hat{\mathbf{s}} \cdot \hat{\mathbf{s}}' \mathrm{d}\Omega$ and is an anisotropic parameter. If $g = 0$, then there is only isotropic scattering.

Using the phenomenological phase function, the transport equation can be written as

$$\hat{\mathbf{s}} \cdot \nabla f(\mathbf{r}, \hat{\mathbf{s}}) = -\gamma_{tr} f(\mathbf{r}, \hat{\mathbf{s}}) + \frac{\gamma_s'}{4\pi} \int_{(4\pi)} f(\mathbf{r}, \hat{\mathbf{s}}') \, \mathrm{d}\Omega' \tag{43}$$

where the transport coefficient, γ_{tr} is defined by

$$\gamma_{tr} = \gamma_s' + \gamma_a, \tag{44}$$

with the effective scattering coefficient $\gamma_s' = \gamma_s(1 - g)$. The transport coefficient is the inverse of the transport mean free path $l^* = 1/\gamma_{tr}$, which is the distance over which the photon's velocity relaxes, and is proportional to the papers optical thickness $\tau = t/l^* = \gamma_{tr} t$. The optical thickness is the ratio of the paper's thickness to the mean free path.

The photon distribution can be separated into two parts: a term representing the unscattered and forward scattered injected photons $f_i(\mathbf{r}, \hat{\mathbf{s}})$ and a term that represents the (nearly) diffuse scattered photons $f_d(\mathbf{r}, \hat{\mathbf{s}})$. The injected distribution is the source of the diffuse photons and satisfies (from Equation 43):

$$\frac{\mathrm{d}}{\mathrm{d}z} f_i(\mathbf{r}, \hat{\mathbf{s}}) = -\gamma_{tr} f_i(\mathbf{r}, \hat{\mathbf{s}}) \tag{45}$$

The solution to this equation with the boundary conditions indicated earlier is

$$f_i(\mathbf{r}, \hat{\mathbf{s}}) = \frac{S_0 \delta(\rho)}{2\pi c \rho} \exp\ (-\gamma_{tr} z) \delta(1 - \hat{\mathbf{s}} \cdot \hat{\mathbf{x}}_3) \tag{46}$$

Handbook of Digital Imaging, Online © 2015 John Wiley & Sons, Ltd.

This article was published in the *Handbook of Digital Imaging* in 2015 by John Wiley & Sons, Ltd.
DOI: 10.1002/9781118798706.hdi052

where $\hat{\mathbf{x}}_3$ is a unit vector in the $+z$ direction, and S_0 is the number of photons per unit time injected.

The transport equation for the diffuse photon

$$\hat{\mathbf{s}} \cdot \nabla f_{\mathrm{d}}(\mathbf{r}, \hat{\mathbf{s}}) = -\gamma_{\mathrm{tr}} f_{\mathrm{d}}(\mathbf{r}, \hat{\mathbf{s}}) + \frac{\gamma_{\mathrm{s}}'}{4\pi} \int_{(4\pi)} f_{\mathrm{d}}(\mathbf{r}, \hat{\mathbf{s}}')\ \mathrm{d}\Omega' + \frac{1}{4\pi c} S(\mathbf{r}) \tag{47}$$

where the source term for the diffuse photons is

$$\begin{aligned} S(\mathbf{r}) &= c\gamma_{\mathrm{s}}' \int_{(4\pi)} f_{\mathrm{i}}(\mathbf{r}, \hat{\mathbf{s}}')\, \mathrm{d}\Omega' \\ &= \frac{\gamma_{\mathrm{s}}' S_0 \delta(\rho)}{2\pi\rho} \exp(-\gamma_{\mathrm{tr}} z). \end{aligned} \tag{48}$$

One makes the diffusion, or P_1 approximation [28] by expanding the photon distribution in spherical harmonics and keeping the first four terms, the $l = 0$, $m = 0$, and the $l = 1$, $m = -1, 0, 1$ terms. One can write

$$f_{\mathrm{d}}(\mathbf{r}, \hat{\mathbf{s}}) = \sum_{lm} q_{lm}(\mathbf{r}) Y_{lm}(\theta, \phi) \tag{49}$$

where $Y_{lm}(\theta, \phi)$ are spherical harmonics [40], and

$$q_{lm}(\mathbf{r}) = \int_{(4\pi)} f_{\mathrm{d}}(\mathbf{r}, \hat{\mathbf{s}}) Y_{lm}^*(\theta, \phi) \mathrm{d}\Omega \tag{50}$$

Expanding $f_{\mathrm{d}}(\mathbf{r}, \hat{\mathbf{s}})$ to the first four terms one finds

$$f_{\mathrm{d}}(\mathbf{r}, \hat{\mathbf{s}}) = q_{00} Y_{00}(\theta, \phi) + q_{1-1} Y_{1-1}(\theta, \phi) + q_{10} Y_{10}(\theta, \phi) + q_{11} Y_{11}(\theta, \phi) \tag{51}$$

and writing the spherical harmonics explicitly one gets

$$\begin{aligned} f_{\mathrm{d}}(\mathbf{r}, \hat{\mathbf{s}}) = {} & \frac{1}{2\sqrt{\pi}} q_{00} \\ & + \sqrt{\frac{3}{8\pi}} q_{1-1} \sin\theta \exp(-i\phi) + \sqrt{\frac{3}{4\pi}} q_{1\ 0} \cos\theta \\ & - \sqrt{\frac{3}{8\pi}} q_{1\ 1} \sin\theta \exp(i\phi). \end{aligned} \tag{52}$$

Defining

$$q_0 = \frac{1}{\sqrt{4\pi}} q_{00}, \quad q_1 = \sqrt{\frac{3}{2\pi}} (q_{1-1} - q_{11}), \quad q_2 = i\sqrt{\frac{3}{2\pi}} (q_{1-1} + q_{11}), \quad q_3 = \sqrt{\frac{3}{4\pi}} q_{10},$$

where $q_1,\ q_2,\ q_3$ are defined as the x, y, z components of the vector $\mathbf{q}(\mathbf{r})$. One can then write Equation 52 as

$$f_{\mathrm{d}}(\mathbf{r}, \hat{\mathbf{s}}) = q_0(\mathbf{r}) + q_1(\mathbf{r}) \sin\theta \cos\phi + q_2(\mathbf{r}) \sin\theta \sin\phi + q_3(\mathbf{r}) \cos\theta \tag{53}$$

Handbook of Digital Imaging, Online © 2015 John Wiley & Sons, Ltd.

This article was published in the *Handbook of Digital Imaging* in 2015 by John Wiley & Sons, Ltd.
DOI: 10.1002/9781118798706.hdi052

or

$$f_{\mathrm{d}}(\mathbf{r}, \hat{\mathbf{s}}) = q_0(\mathbf{r}) + \mathbf{q}(\mathbf{r}) \cdot \hat{\mathbf{s}}, \tag{54}$$

with

$$\hat{\mathbf{s}} = \hat{\mathbf{x}}_i s_i \tag{55}$$

where a summation over the repeated index i is implied, $\hat{\mathbf{x}}_1, \hat{\mathbf{x}}_2, \hat{\mathbf{x}}_3$ are unit vectors along the x, y, z axes respectively, and s_1, s_2, s_3 are the x, y, z components of the vector $\hat{\mathbf{s}}$:

$$s_1 = \sin\theta\cos\phi, \quad s_2 = \sin\theta\sin\phi, \quad s_3 = \cos\theta \tag{56}$$

In the following explicit expressions for q_0 and $\mathbf{q}$ are obtained.

The diffuse photon density $u(\mathbf{r})$ (number of photons per unit volume) at position $\mathbf{r}$ is obtained by integrating f_{d} over 4π solid angle:

$$u(\mathbf{r}) = \int_{4\pi} f_{\mathrm{d}}(\mathbf{r}, \hat{\mathbf{s}})\, \mathrm{d}\Omega. \tag{57}$$

Substituting the expression for f_{d}, Equation 54, or equivalently Equation 53, into Equation 57, one obtains the diffuse photon density $u(\mathbf{r})$. The integral of the second term on the right-hand side in Equation 54 is identically zero as

$$\int_{4\pi} \cos\theta\, \mathrm{d}\Omega = \int_{4\pi} \sin\theta\cos\phi\, \mathrm{d}\Omega = \int_{4\pi} \sin\theta\sin\phi\, \mathrm{d}\Omega = 0. \tag{58}$$

The integral of the first term on the right-hand side in Equation 54 gives

$$q_0(\mathbf{r}) = \frac{1}{4\pi} u(\mathbf{r}). \tag{59}$$

The diffuse photon current density (number of photons per unit area per unit time) at position $\mathbf{r}$ is $\mathbf{j}(\mathbf{r})$ is given by

$$\mathbf{j}(\mathbf{r}) = c \int_{4\pi} f_{\mathrm{d}}(\mathbf{r}, \hat{\mathbf{s}})\, \hat{\mathbf{s}} \mathrm{d}\Omega. \tag{60}$$

As $\int_{4\pi} \hat{\mathbf{s}}\, \mathrm{d}\Omega = 0$, the integral Equation 60 using the first term on the right-hand side in Equation 54 is zero. Integrating Equation 60 using the second term in Equation 54, one obtains

$$\begin{aligned} \int_{4\pi} \mathbf{q} \cdot \hat{\mathbf{s}}\, \hat{\mathbf{s}}\, \mathrm{d}\Omega &= \int_{4\pi} (q_i s_i)(\hat{\mathbf{x}}_k s_k)\, \mathrm{d}\Omega \\ &= \hat{\mathbf{x}}_k q_i \int_{4\pi} s_i s_k \mathrm{d}\Omega = \frac{4\pi}{3}\mathbf{q} \end{aligned} \tag{61}$$

where summation over repeated indices is assumed and it is easily shown that

$$\int s_i\, s_j \mathrm{d}\Omega = \frac{4\pi}{3}\delta_{ij}. \tag{62}$$

One sees that

$$\mathbf{q}(\mathbf{r}) = \frac{3}{4\pi c}\mathbf{j}(\mathbf{r}). \tag{63}$$

Handbook of Digital Imaging, Online © 2015 John Wiley & Sons, Ltd.
This article is © 2015 John Wiley & Sons, Ltd.
This article was published in the *Handbook of Digital Imaging* in 2015 by John Wiley & Sons, Ltd.
DOI: 10.1002/9781118798706.hdi052

The expression for f_d, Equation 51, becomes:

$$f_d(\mathbf{r}, \hat{\mathbf{s}}) = \frac{1}{4\pi} u(\mathbf{r}) + \frac{3}{4\pi c} \mathbf{j}(\mathbf{r}) \cdot \hat{\mathbf{s}}. \tag{64}$$

To get the diffusion equation, one first integrates Equation 47 over all solid angles to get a continuity equation:

$$\int \hat{\mathbf{s}} \cdot \nabla f_d(\mathbf{r}, \hat{\mathbf{s}}) d\Omega = -\gamma_{tr} \int f_d(\mathbf{r}, \hat{\mathbf{s}}) d\Omega + \frac{\gamma_s'}{4\pi} \iint f_d(\mathbf{r}, \hat{\mathbf{s}}') d\Omega' d\Omega + \frac{1}{4\pi c} \int S(\mathbf{r}) d\Omega \tag{65}$$

The term on the left-hand side of Equation 65 can be written as

$$\frac{1}{4\pi} \int s_i \partial_i (u + 3c^{-1} j_k s_k) d\Omega = \frac{1}{4\pi} \left[\partial_i u \int s_i d\Omega + 3c^{-1} \partial_i j_k \int s_i s_k d\Omega \right], \tag{66}$$

where one assumes a sum over repeated indices, and $\partial_i = \partial / \partial x_i$ with $(x_1, x_2, x_3) = (x, y, z)$. The integral over s_i is zero, by Equation 58, and the integral over $s_i s_j$ is $4\pi\delta_{ij}/3$, Equation 62, so one obtains for the first term on the left-hand side of Equation 65:

$$\frac{1}{c} \partial_i j_i = \frac{1}{c} \nabla \cdot \mathbf{j}(\mathbf{r}). \tag{67}$$

The first and second terms on the right side of Equation 65 are easily shown to be $-\gamma_{tr} u$ and $\gamma_s' u$, respectively where Equation 58 is used. The last term on the right-hand side of Equation 65 is trivially shown to be $c^{-1} S$. Combining the terms, one gets for Equation 65:

$$\nabla \cdot \mathbf{j}(\mathbf{r}) = S(\mathbf{r}) - c\gamma_a u(\mathbf{r}) \tag{68}$$

which is a continuity equation. The rate of flow of photons into the point $\mathbf{r}$ is increased by the source photons S at that point and decreased by absorption.

To get the diffusion equation, one must also multiply Equation 47 by $\hat{\mathbf{s}}$ and integrate over all solid angles. The term on the left-hand side of Equation 47 becomes

$$\int \hat{\mathbf{s}}\, \hat{\mathbf{s}} \cdot \nabla f_d(\mathbf{r}, \hat{\mathbf{s}}) d\Omega = \frac{1}{4\pi} \int \hat{\mathbf{s}} [\hat{\mathbf{s}} \cdot \nabla u + 3c^{-1} \hat{\mathbf{s}} \cdot \nabla (\mathbf{j} \cdot \hat{\mathbf{s}})] d\Omega \tag{69}$$

The first term on the right-hand side above, Equation 69, can be written as

$$\frac{1}{4\pi} \int \hat{\mathbf{x}}_i s_i (s_j \partial_j u) d\Omega = \frac{1}{4\pi} \hat{\mathbf{x}}_i \partial_j u \int s_i s_j d\Omega \tag{70}$$

which is

$$\hat{\mathbf{x}}_i \partial_j u \frac{1}{3} \delta_{ik} = \frac{1}{3} \nabla u \tag{71}$$

Handbook of Digital Imaging, Online © 2015 John Wiley & Sons, Ltd.

This article was published in the *Handbook of Digital Imaging* in 2015 by John Wiley & Sons, Ltd.
DOI: 10.1002/9781118798706.hdi052

using Equation 62. The second integral on the right in Equation 69 can be written as

$$\int \hat{\mathbf{x}}_i s_i [s_j \partial_j (j_k s_k)] \mathrm{d}\Omega = \hat{\mathbf{x}}_i \partial_j j_k \int s_i s_j s_k \mathrm{d}\Omega. \tag{72}$$

In the following, it is shown that the integral over $s_i s_j s_k$ is always zero. The integral can be written as

$$\int_0^{\pi} \cos^n\theta \sin^{m+1}\theta \, \mathrm{d}\theta \int_0^{2\pi} \cos^{n'}\phi \sin^{m'}\phi \mathrm{d}\phi \tag{73}$$

with $n + m = 3$. If n is odd, then it is easily shown that the integral over θ is zero. If n is even, then it is either 0 or 2. If $n = 0$, then $n' + m' = 3$ so that one of them is even and the other odd, and it is easily shown that the integral over ϕ is zero. If $n = 2$, then $n' + m' = 1$ and again it is easy to show that the integral over ϕ is zero. One obtains for the integral, Equation 69:

$$\frac{1}{3}\nabla u(\mathbf{r}). \tag{74}$$

Multiplying $\hat{\mathbf{s}}$ times the first term on the right-hand side of Equation 47 and integrating over all solid angles:

$$-\gamma_{\mathrm{tr}} \int_{4\pi} f_{\mathrm{d}}(\mathbf{r}, \hat{\mathbf{s}}) \hat{\mathbf{s}} \mathrm{d}\Omega = -\frac{\gamma_{\mathrm{tr}}}{c} \mathbf{j}(\mathbf{r}), \tag{75}$$

by Equation 60, and multiplying $\hat{\mathbf{s}}$ times the second and third terms in Equation 47 and integrating over all solid angles, one finds that both integrals are zero by Equation 58. One obtains

$$\mathbf{j}(\mathbf{r}) = -\frac{c}{3\gamma_{\mathrm{tr}}} \nabla u(\mathbf{r}). \tag{76}$$

This expression characterizes the diffusion approximation – the photon current is due to only the gradient in the photon density.

Taking the divergence of Equation 76 and equating its right-hand side with the right-hand side of Equation 68, one obtains the diffusion equation:

$$D\nabla^2 u(\mathbf{r}) - c\gamma_{\mathrm{a}} u(\mathbf{r}) = S(\mathbf{r}), \tag{77}$$

with the diffusion constant D given by

$$D = \frac{l^* c}{3} \tag{78}$$

where l^* is the mean free path. In the following, using appropriate boundary condition, this equation is solved by constructing a Green's function.

Handbook of Digital Imaging, Online © 2015 John Wiley & Sons, Ltd.

This article was published in the *Handbook of Digital Imaging* in 2015 by John Wiley & Sons, Ltd.
DOI: 10.1002/9781118798706.hdi052

3.2 Boundary Conditions

There are two boundaries, the top surface of the paper and the bottom surface. (Note that the $+z$ axis is pointing downward.) Photons are normally incident on the paper top surface at the origin. Away from the origin, there is no inward photon flux, only an outward flux, through both top and bottom, of internally scattered and diffusing photons. There is, however, some internal reflection at the boundaries. This internal reflection can be considered an inward traveling flux equal to the outward flux times the Fresnel reflectance [34].

One can define the partial photon currents $\mathbf{j}_+(\rho, z)$ and $\mathbf{j}_-(\rho, z)$ as

$$\mathbf{j}_+(\rho, z) = c \int_{0 \le \theta \le \pi/2} f_{\mathrm{d}}(\rho, z; \hat{\mathbf{s}}) \hat{\mathbf{s}} \, \mathrm{d}\Omega \tag{79}$$

as the downward photon current and

$$\mathbf{j}_-(\rho, z) = c \int_{\pi/2 \le \theta \le \pi} f_{\mathrm{d}}(\rho, z; \hat{\mathbf{s}}) \hat{\mathbf{s}} \, \mathrm{d}\Omega \tag{80}$$

as the upward photon current, with $\mathbf{j}(\rho, z) = \mathbf{j}_+(\rho, z) + \mathbf{j}_-(\rho, z)$. Using Equation 64 in Equations 79 and 80, one obtains

$$\mathbf{j}_\pm(\rho, z) = \pm \frac{c}{4} \, u(\rho, z) \hat{\mathbf{x}}_3 + \frac{1}{2} \mathbf{j}(\rho, z) \tag{81}$$

or, using Equation 76

$$\mathbf{j}_\pm(\rho, z) = \pm \frac{c}{4} \, u(\rho, z) \hat{\mathbf{x}}_3 - \frac{D}{2} \nabla u(\rho, z) \tag{82}$$

with $\hat{\mathbf{x}}_3$ a unit vector pointing in the $+z$ direction.

As indicated earlier, there is no external inward flux except at the origin. However, the internally reflected outward flux can be treated as an inward flux at the boundary, that is, the flux directed inward at the paper surface is equal to the reflected part of the outwardly directed flux [30]. It can be shown that this internal reflection can be characterized by an effective Fresnel reflection coefficient, R_{F} [3]. The boundary conditions are

$$\hat{\mathbf{x}}_3 \cdot \mathbf{j}_+(\rho, 0) = -R_{\mathrm{F}} \hat{\mathbf{x}}_3 \cdot \mathbf{j}_-(\rho, 0) \tag{83}$$

for the top surface and the bottom surface:

$$\hat{\mathbf{x}}_3 \cdot \mathbf{j}_-(\rho, t) = -R_{\mathrm{F}} \hat{\mathbf{x}}_3 \cdot \mathbf{j}_+(\rho, t). \tag{84}$$

Using Equation 82, this becomes

$$\frac{c}{4} u(\rho, 0) - \frac{D}{2} \frac{\partial}{\partial z} u(\rho, z)|_{z=0} = R_{\mathrm{F}} \left[\frac{c}{4} u(\rho, 0) + \frac{D}{2} \frac{\partial}{\partial z} u(\rho, z)|_{z=0} \right] \tag{85}$$

for the top surface, and

$$-\frac{c}{4} u(\rho, t) - \frac{D}{2} \frac{\partial}{\partial z} u(\rho, z)|_{z=t} = -R_{\mathrm{F}} \left[\frac{c}{4} u(\rho, t) + \frac{D}{2} \frac{\partial}{\partial z} u(\rho, z)|_{z=t} \right] \tag{86}$$

Handbook of Digital Imaging, Online © 2015 John Wiley & Sons, Ltd.

This article was published in the *Handbook of Digital Imaging* in 2015 by John Wiley & Sons, Ltd.
DOI: 10.1002/9781118798706.hdi052

for the bottom surface. Thus, one obtains a mixed homogeneous boundary condition for the top surface:

$$u(\rho, 0) - \alpha \frac{\partial}{\partial z} u(\rho, z)|_{z=0} = 0 \tag{87}$$

and for the bottom surface:

$$u(\rho, t) + \alpha \frac{\partial}{\partial z} u(\rho, z)|_{z=t} = 0 \tag{88}$$

where

$$\alpha = \frac{2l^*}{3} \frac{1 + R_F}{1 - R_F}. \tag{89}$$

3.3 Green's Function Solution

In the following, a Green's function is developed to solve Equation 77. Let $\mathcal{L}$ be an arbitrary linear differential operator acting on $\mathbf{r}$. It is easily shown that if

$$\mathcal{L}u(\mathbf{r}) = f(\mathbf{r}) \tag{90}$$

and there is a Green's function G such that

$$\mathcal{L}G(\mathbf{r}, \mathbf{r}') = \delta(\mathbf{r} - \mathbf{r}') \tag{91}$$

then

$$u(\mathbf{r}) = \int f(\mathbf{r}')G(\mathbf{r}, \mathbf{r}')\mathrm{d}^3 r' \tag{92}$$

That this is the case is shown by operating on both sides with $\mathcal{L}$:

$$\mathcal{L}u(\mathbf{r}) = \int f(\mathbf{r}')\mathcal{L}G(\mathbf{r}, \mathbf{r}')\mathrm{d}^3 r' = \int f(\mathbf{r}')\delta(\mathbf{r} - \mathbf{r}')\mathrm{d}^3 r' = f(\mathbf{r}) \tag{93}$$

which is precisely Equation 90. In the case treated here, $\mathcal{L} = \nabla^2 - k^2$ with $k = \sqrt{c\gamma_a/D}$ and the source term $f(\mathbf{r}) = -D^{-1}S(\mathbf{r})$. Using cylindrical coordinates, one writes for ∇^2

$$\nabla^2 = L_\rho + L_z, \tag{94}$$

where

$$L_\rho = \frac{1}{\rho} \frac{\partial}{\partial \rho} \rho \frac{\partial}{\partial \rho} \tag{95}$$

and

$$L_z = \frac{\partial^2}{\partial z^2}. \tag{96}$$

Handbook of Digital Imaging, Online © 2015 John Wiley & Sons, Ltd.

This article was published in the *Handbook of Digital Imaging* in 2015 by John Wiley & Sons, Ltd.
DOI: 10.1002/9781118798706.hdi052

Owing to the symmetry, $\partial G/\partial\theta = 0$. The equation for G becomes

$$(L_\rho + L_z - k^2)G(\rho, \rho'; z, z') = -\frac{\delta(\rho - \rho')\delta(z - z')}{2\pi\rho}. \tag{97}$$

One can write G as

$$G(\rho, \rho'; z, z') = \sum_n g_n(\rho, \rho')\psi_n(z)\psi_n(z') \tag{98}$$

where $\psi_n(z)$ are orthonormal basis functions that satisfy

$$L_z\psi_n(z) = -\mu_n^2\psi_n(z) \tag{99}$$

which are

$$\psi_n(z) = A_n \sin(\mu_n z + \lambda_n), \tag{100}$$

where it is easily shown by integrating $|\psi_n(z)|^2$ between 0 and t that

$$A_n = \left[\frac{4\mu_n}{2\mu_n - \sin[2(\mu_n t + \lambda_n)] + \sin(2\lambda_n)}\right]^{1/2}. \tag{101}$$

With the boundary conditions given by Equations 87 and 88, one can evaluate the eigenvalues and phases μ_n and λ_n. At $z = 0$, one finds for Equation 87

$$\sin\lambda_n - \alpha\mu_n\cos\lambda_n = 0 \tag{102}$$

or

$$\tan\lambda_n = \alpha\mu_n. \tag{103}$$

At $z = t$, Equation 88 can be written as

$$\sin(\mu_n t + \lambda_n) + \alpha\mu_n\cos(\mu_n t + \lambda_n) \tag{104}$$

or

$$\tan(\mu_n t + \lambda_n) = -\alpha\mu_n. \tag{105}$$

Using $\tan(x + y) = (\tan x + \tan y)/(1 - \tan x \tan y)$, one obtains an equation for μ_n:

$$\tan(\mu_n t) = \frac{2\alpha\mu_n}{(\alpha\mu_n)^2 - 1}, \tag{106}$$

which must be solved numerically. A fast algorithm for calculating μ_n and λ_n is given in Appendix.

Using Equations 103 and 105, one sees that

$$\tan\lambda_n = -\tan(\mu_n t + \lambda_n) \tag{107}$$

As $\tan x = \tan(x + n\pi)$ and $-\tan x = \tan(-x)$, this can be written as

$$\mu_n t = n\pi - 2\lambda_n. \tag{108}$$

Handbook of Digital Imaging, Online © 2015 John Wiley & Sons, Ltd.

This article was published in the *Handbook of Digital Imaging* in 2015 by John Wiley & Sons, Ltd.
DOI: 10.1002/9781118798706.hdi052

As $n \to \infty$ it follows that $\lambda_n \to \pi/2$ and $\mu_n \to (n-1)\pi$. Using this result, the normalization factor takes a simpler form:

$$A_n = \left[\frac{2\mu_n}{\mu_n t + \sin 2\lambda_n}\right]^{1/2} \tag{109}$$

Equation 97 can then be written as

$$\sum_n \psi_n(z)\psi_n(z')L_\rho g_n(\rho,\rho') - \sum_n g_n(\rho,\rho')(\mu_n^2 + k^2)\psi_n(z)\psi_n(z') = -\frac{\delta(\rho-\rho')\delta(z-z')}{2\pi\rho}. \tag{110}$$

Multiplying both sides of Equation 110 by $\psi_m(z)$ and integrating over z between 0 and t one finds

$$\frac{\partial}{\partial\rho}\rho\frac{\partial}{\partial\rho}g_m(\rho,\rho') - (\mu_n^2 + k^2)\rho g_m(\rho,\rho') = -\frac{1}{2\pi}\delta(\rho-\rho'). \tag{111}$$

This is the modified Helmholtz equation [40] and has solutions $K_0(\sigma_n\rho)$ and $I_0(\sigma_n\rho)$, where K_0 and I_0 are modified Bessel functions of zero order, and

$$\sigma_n^2 = \mu_n^2 + k^2 = \mu_n^2 + c\gamma_a/D = \mu_n^2 + 3\gamma_a\gamma_{tr}. \tag{112}$$

One is interested in the region $\rho > 0$; as seen in the expression for the source term, Equation 48, ρ' is identically 0, and one requires that g_n goes to zero as $\rho \to \infty$ so that one chooses

$$g_n(\rho,\rho') = K_0(\sigma_n\rho)I_0(\sigma_n\rho') \quad \rho > \rho' \tag{113}$$

Then, the complete solution is

$$G(\rho,\rho';z,z') = \sum_n \psi_n(z)\psi_n(z')I_0(\sigma_n\rho')K_0(\sigma_n\rho). \tag{114}$$

Substituting the expression for G into Equation 92 with $f(\mathbf{r}) = -D^{-1}S(\mathbf{r})$ with $S(\mathbf{r})$ given by Equation 48, one gets

$$u(\mathbf{r}) = D^{-1}\int S(\rho',z')G(\rho,\rho';z,z')\rho'\mathrm{d}\rho'\mathrm{d}z'. \tag{115}$$

The integral over ρ' is trivial, and integrating over z' one must solve the following integral:

$$\int_0^t \sin(\mu_n z' + \lambda_n)\exp(-\gamma_{tr}z')\mathrm{d}z'. \tag{116}$$

It can be evaluated in a straightforward way to get

$$\frac{1}{\mu_n^2 + \gamma_{tr}^2}[\gamma_{tr}\sin\lambda_n + \mu_n\cos\lambda_n - \{\gamma_{tr}\sin(\mu_n t + \lambda_n) + \mu_n\cos(\mu_n t + \lambda_n)\}\exp(-\gamma_{tr}t)] \tag{117}$$

Handbook of Digital Imaging, Online © 2015 John Wiley & Sons, Ltd.

This article was published in the *Handbook of Digital Imaging* in 2015 by John Wiley & Sons, Ltd.
DOI: 10.1002/9781118798706.hdi052

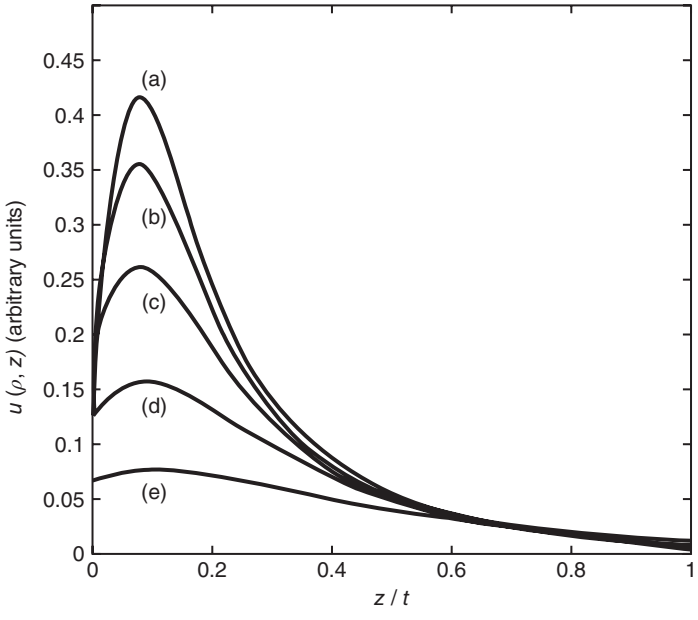

Figure 3 Photon density as a function of distance into the paper for several values of $\tau = \gamma_{tr} t$ with t held constant. (a) $\tau = 80$, (b) $\tau = 32$, (c) $\tau = 16$, (d) $\tau = 8$, and (e) $\tau = 4$

Using Equation 108, one sees that $\sin(\mu_n t + \lambda_n) = (-1)^{n+1} \sin \lambda_n$ and $\cos(\mu_n t + \lambda_n) = (-1)^n \cos \lambda_n$. From Equation 88, it is apparent that $\gamma_{tr} \sin \lambda_n = w \mu_n \cos \lambda_n$, where $w = \gamma_{tr} \alpha$ and α is given by Equation 89. The integral Equation 117 can be written as

$$\frac{\mu_n \cos \lambda_n}{\mu_n^2 + \gamma_{tr}^2} [1 + w + (-1)^n (1 - w) \exp(-\gamma_{tr} t)]. \tag{118}$$

Using the fact that $\sin 2\lambda = 2 \sin \lambda \cos \lambda$, one obtains for the photon density:

$$u(\rho, z) = \frac{3 S_0 w}{2\pi c} \sum_n \frac{\Gamma_n}{\sin \lambda_n} \sin(\mu_n z + \lambda_n) \, K_0(\sigma_n \rho) \tag{119}$$

where

$$\Gamma_n = \frac{\gamma_s' \gamma_{tr}}{\mu_n^2 + \gamma_{tr}^2} \frac{\mu_n^2 \sin 2\lambda_n}{\mu_n t + \sin 2\lambda_n} [(1 + w^{-1}) + (-1)^n (1 - w^{-1}) \exp(-\gamma_{tr} t)]. \tag{120}$$

Figure 3 shows $u(\rho, z)$ for several values $\tau = \gamma_{tr} t$.

4 Diffusion Point Spread Function

The diffusion PSF is equal to the normalized diffuse photon flux through the top surface of the paper as a function of the distance from the point of incidence. This is obtained from the

Handbook of Digital Imaging, Online © 2015 John Wiley & Sons, Ltd.

This article was published in the *Handbook of Digital Imaging* in 2015 by John Wiley & Sons, Ltd.
DOI: 10.1002/9781118798706.hdi052

partial diffuse photon current in the $-z$ direction given by Equation 80 at $z = 0$. The diffuse photon flux through the top surface is

$$F_{-}(\rho) = -(1 - R_{\mathrm{F}})\hat{\mathbf{x}}_3 \cdot \mathbf{j}_{-}(\rho, 0). \tag{121}$$

From Equation 82, one sees that

$$\hat{\mathbf{x}}_3 \cdot \mathbf{j}_{-}(\rho, 0) = -\frac{c}{4}u(\rho, 0) - \frac{D}{2}\frac{\partial}{\partial z}u(\rho, 0). \tag{122}$$

Using the boundary condition Equation 87, the right-hand side can be written

$$-\frac{c}{4}u(\rho, 0) - \frac{D}{2\alpha}u(\rho, 0) = -\frac{c}{2}\frac{1}{1 + R_{\mathrm{F}}}u(\rho, 0), \tag{123}$$

where Equations 78 and 89 have been used for D and α. The diffuse photon flux can then be written as

$$F_{-}(\rho) = \frac{c}{2}\frac{1 - R_{\mathrm{F}}}{1 + R_{\mathrm{F}}}u(\rho, 0). \tag{124}$$

The diffuse reflectance of the paper is the total diffuse flux out divided by the flux in, S_0:

$$R_{\mathrm{p}} = S_0^{-1}\int F_{-}(\rho)\mathrm{d}A = \frac{c}{2S_0}\frac{1 - R_{\mathrm{F}}}{1 + R_{\mathrm{F}}}2\pi\int_0^{\infty} u(\rho, 0)\rho\mathrm{d}\rho. \tag{125}$$

Using Equation 57 for $u(\rho, 0)$, the integral over K_0 evaluates as σ_n^{-2}. Noting that $\psi_n(0) = A_n \sin\lambda_n$ and that $w^{-1} = 3/2(1 - R_{\mathrm{F}})/(1 + R_{\mathrm{F}})$, the paper's reflectance can be written as

$$R_{\mathrm{p}} = \sum_n \Gamma_n \sigma_n^{-2}. \tag{126}$$

The paper's PSF is the normalized diffuse photon flux out of the surface:

$$H(\rho) = \frac{F_{-}(\rho)}{2\pi\int_0^{\infty} F_{-}(\rho)\rho\mathrm{d}\rho} \tag{127}$$

or

$$H(\rho) = \frac{1}{2\pi R_{\mathrm{p}}}\sum_n \Gamma_n K_0(\sigma_n\rho). \tag{128}$$

The normalized diffusion LSF is obtained integrating the PSF over y:

$$L(x) = \int_{\infty}^{-\infty} H(\sigma_n\sqrt{x^2 + y^2})\mathrm{d}y. \tag{129}$$

One obtains

$$L(x) = \frac{1}{2R_{\mathrm{p}}}\sum_n \Gamma_n \sigma_n^{-1}\exp\left(-\sigma_n|x|\right). \tag{130}$$

Handbook of Digital Imaging, Online © 2015 John Wiley & Sons, Ltd.

This article was published in the *Handbook of Digital Imaging* in 2015 by John Wiley & Sons, Ltd.
DOI: 10.1002/9781118798706.hdi052

The MTF is readily found by taking the Fourier transform of $L(x)$:

$$\tilde{H}(\omega) = \frac{1}{R_\mathrm{p}} \sum_n \frac{\Gamma_n}{(2\pi\omega)^2 + \sigma_n^2} \tag{131}$$

Using the definition Equation 132, one can write $\tilde{H}_k$ as

$$\tilde{H}_k = \frac{1}{2R_\mathrm{p}} \sum_n \frac{\Gamma_n}{(2\pi/r)^2 k + \sigma_n^2}. \tag{132}$$

The MTF is shown in Figure 4 for several values of $\tau = t/l^* = \gamma_\mathrm{tr} t$.

The diffusion length, defined as the average distance a photon diffuses within the paper is given by Equation 32 and is found to be

$$\bar{\rho} = \frac{\pi}{2R_\mathrm{p}} \sum_n \Gamma_n \sigma_n^{-3}. \tag{133}$$

As indicated earlier, $\bar{\rho}^{-1}$ is approximately the spatial bandwidth of the paper. Figure 5 shows a plot of $\bar{\rho}$ in units of mean free path as a function of optical density $\tau = \gamma_\mathrm{tr} t$ for several different γ_a values with thickness held constant. Figure 6 shows $\bar{\rho}$ in units of screen period r as a function of τ.

The halftone reflectance, Equation 25 using Equation 132 for $\tilde{H}_k$ is shown in Figure 7. Also, shown are the reflectances for complete diffusion ($\tau \ll 1$) and for no diffusion ($\tau \gg 1$).

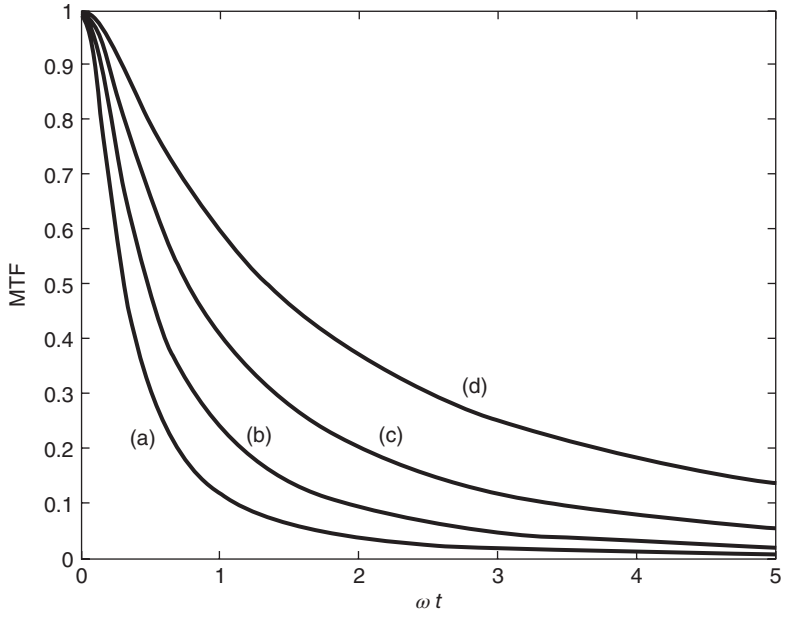

Figure 4 The diffusion MTF. (a) $\tau = 2.5$, (b) $\tau = 5$, (c) $\tau = 10$, and (d) $\tau = 20$

Handbook of Digital Imaging, Online © 2015 John Wiley & Sons, Ltd.

This article was published in the *Handbook of Digital Imaging* in 2015 by John Wiley & Sons, Ltd.
DOI: 10.1002/9781118798706.hdi052

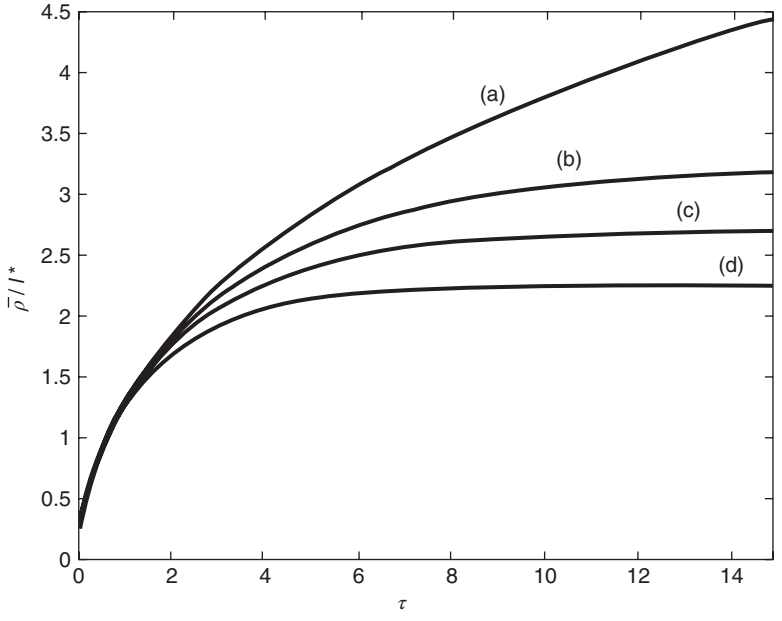

Figure 5 The diffusion length $\bar{\rho}$ in units of mean free path l^* as a function of optical density, mean free path held constant. (a) $\gamma_a/\gamma_s = 0$, (b) $\gamma_a/\gamma_s = 0.1$, (c) $\gamma_a/\gamma_s = 0.2$ (d) $\gamma_a/\gamma_s = 0.4$

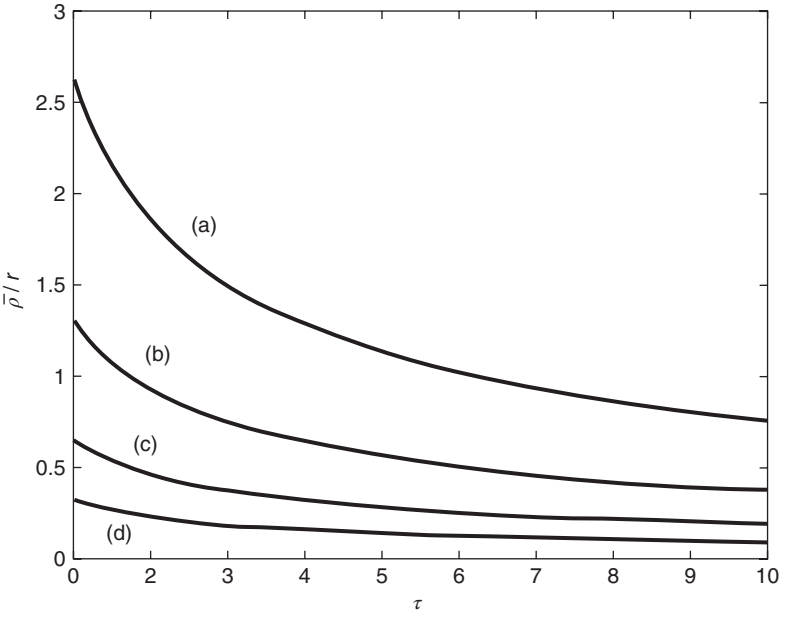

Figure 6 The diffusion length $\bar{\rho}$ in units of screen period r as a function of optical density, paper thickness held constant. (a) $t/r = 2$, (b) $t/r = 1$, (c) $t/r = 0.5$ (d) $t/r = 0.25$

DOI: 10.1002/9781118798706.hdi052

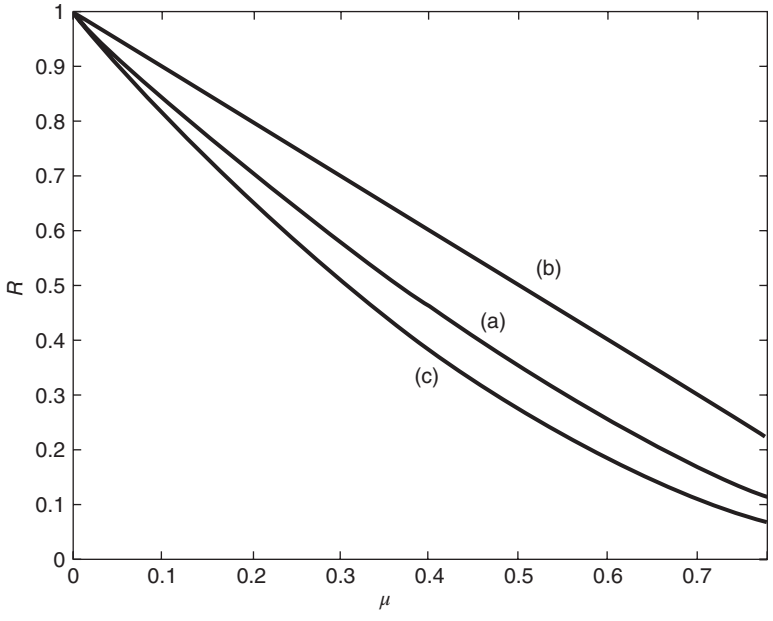

Figure 7 Halftone reflectance: (a) $\tau = 12$, (b) $\tau \gg 1$, and (c) $\tau \ll 1$

4.1 The Diffusion Z-Sum

One is particularly interested in the quantity $\mathcal{Z}$ as this contains the effects of optical dot gain. Using the diffusion MTF, Equation 132, the Z-sum can be written as

$$\mathcal{Z} = \frac{1}{2R_{\mathrm{p}}} \sum_{n=1}^{\infty} \frac{J_1(2\sqrt{\pi k \mu})}{\pi k \mu} \sum_{k=0}^{\infty} \frac{\Gamma_n}{(2\pi/r)^2 k + \sigma_n^2}. \tag{134}$$

As indicated in the discussion before Equations 33 and 39, if $\bar{\rho}/r \gg 1$, then $\mathcal{Z} = 1$ and if $\bar{\rho}/r \ll 1$ then $\mathcal{Z} \approx \mu^{-1}$. This suggests that $\mathcal{Z}$ can be approximated by

$$\mathcal{Z} = \mu^{-s} \tag{135}$$

with

$$0 \leq s \leq 1. \tag{136}$$

Figure 8 shows the halftone reflectance for different values of τ using Equation 134 (line) and using μ^{-s} with $s = 0.7$ for $\mathcal{Z}$. Figure 9 shows $\mu^2 \mathcal{Z}$ and μ^{2-s}.

4.2 Paper Reflectance and Transmittance

The reflectance was calculated previously, Equation 126, and in a similar way the transmittance of the diffuse photons can be calculated –the transmittance is proportional to the photon flux

Handbook of Digital Imaging, Online © 2015 John Wiley & Sons, Ltd.

This article was published in the *Handbook of Digital Imaging* in 2015 by John Wiley & Sons, Ltd.
DOI: 10.1002/9781118798706.hdi052

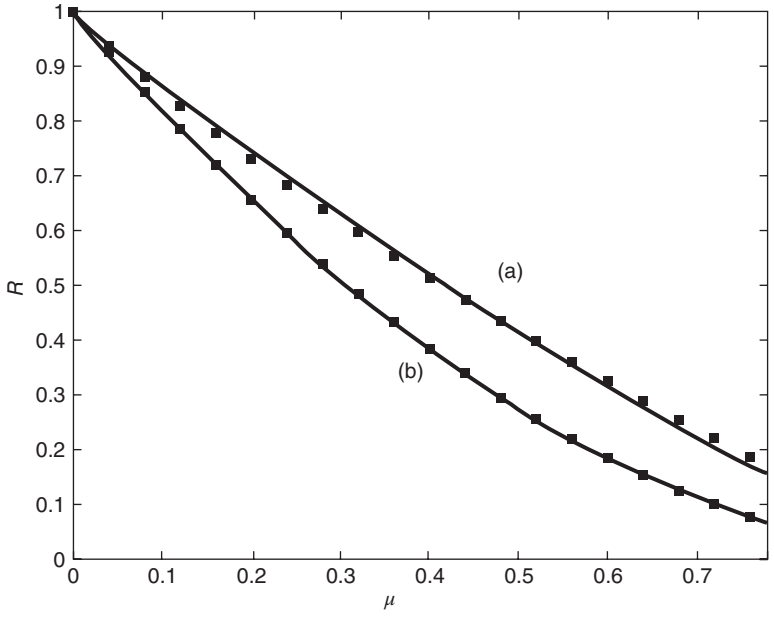

Figure 8 Reflectance calculated using $\mathcal{Z}$ (line) and approximating $\mathcal{Z}$ by μ^{-s} (boxes), with $s = 0.7$ for (a) $\tau = 0$ and (b) $\tau = 40$

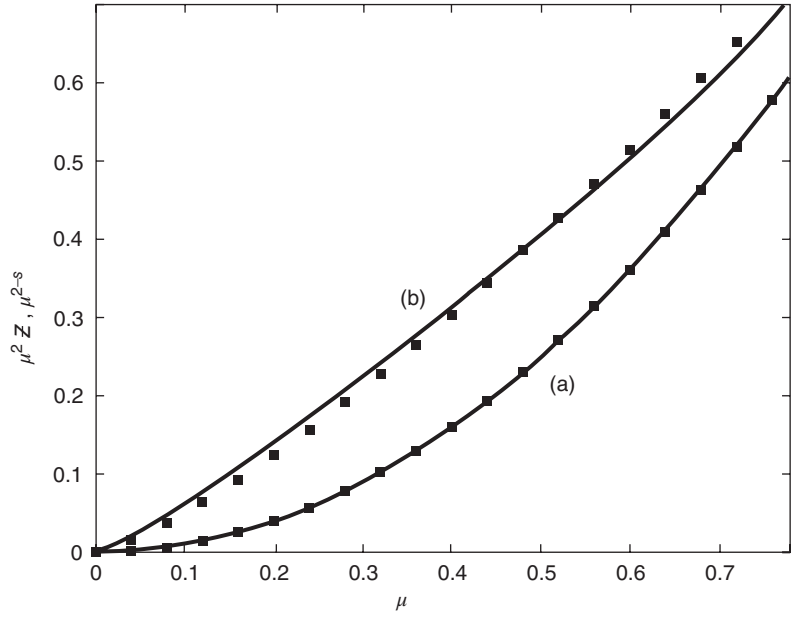

Figure 9 $\mu^2\mathcal{Z}$ (line) and μ^{2-s} (boxes), with $s = 0.7$ for (a) $\tau = 0$ and (b) $\tau = 40$

Handbook of Digital Imaging, Online © 2015 John Wiley & Sons, Ltd.

This article was published in the *Handbook of Digital Imaging* in 2015 by John Wiley & Sons, Ltd.
DOI: 10.1002/9781118798706.hdi052

through the bottom surface of the paper.

$$F_+(\rho) = (1 - R_F)\hat{\mathbf{x}}_3 \cdot \mathbf{j}_+(\rho, t).$$

By Equation 82,

$$\hat{\mathbf{x}}_3 \cdot \mathbf{j}_+(\rho, t) = \frac{c}{4}u(\rho, t) - \frac{D}{2}\frac{\partial}{\partial z}u(\rho, t).$$

Using the boundary condition Equation 88, the right-hand side given previously can be written as

$$\frac{c}{4}u(\rho, t) + \frac{D}{2\alpha}u(\rho, t)$$

which can be written using Equations 78 and 89 for D and α as

$$\frac{c}{2}\frac{1}{1 + R_F}\, u(\rho, t)$$

so the flux through the bottom surface of the paper is

$$F_+(\rho) = \frac{c}{2}\frac{1 - R_F}{1 + R_F}u(\rho, t).$$

The transmittance is the integral of the flux over the area divided by the flux entering the paper, S_0:

$$T_p(\text{diffuse}) = S_0^{-1}\int F_+(\rho)\mathrm{d}A = \frac{c}{2S_0}\frac{1 - R_F}{1 + R_F}2\pi\int_0^\infty u(\rho, t)\rho\mathrm{d}\rho.$$

Noting that $\sin(\mu_n t + \lambda_n) = (-1)^{n+1}\sin(\lambda_n)$ and integrating the previous equation as was done for the reflectance, the transmittance can be written as

$$T_p(\text{diffuse}) = \sum_n (-1)^{n+1}\Gamma_n\sigma_n^{-2}.$$

For $\tau < 1$, however, there will also be transmittance of the injected photons. The transmittance of these photons is

$$T_p(\text{injected}) = \exp\,(-\gamma_{tr}t),$$

and the total transmittance is $T_p = T_p(\text{diffuse}) + T_p(\text{injected})$. The diffuse and injected transmittances are shown in Figure 10, and the reflectance and total transmittance are shown in Figure 11. Both are shown as a function of τ. When $\tau \ll 1$, there are very few diffuse photons –most of the injected light is transmitted – so the diffuse reflectance and transmittance are very small. Figure 10 shows the transmittance of the injected and diffuse photons and Figure 11 shows the total transmittance and the reflectance both as a function of τ.

Handbook of Digital Imaging, Online © 2015 John Wiley & Sons, Ltd.

This article was published in the *Handbook of Digital Imaging* in 2015 by John Wiley & Sons, Ltd.
DOI: 10.1002/9781118798706.hdi052

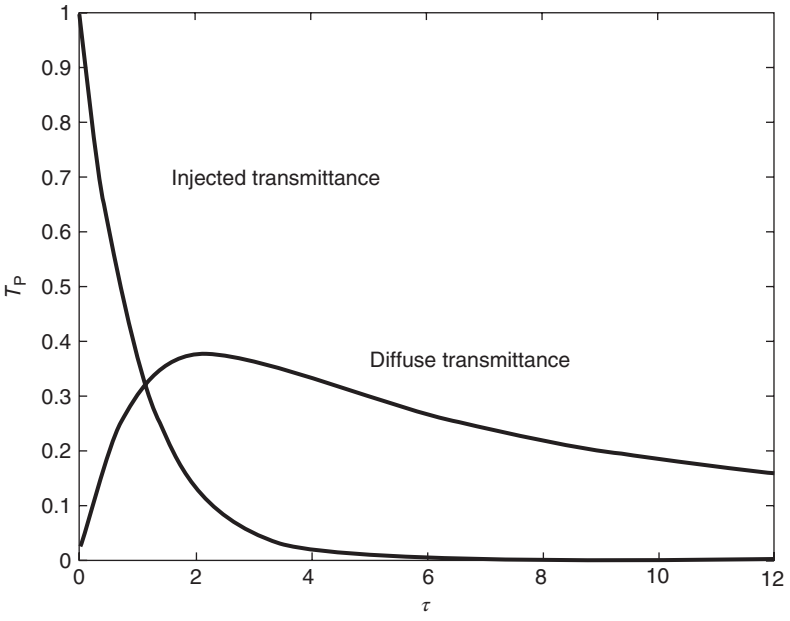

Figure 10 The injected and diffuse transmittances as a function of γ_{tr} with $\gamma_a = 0$

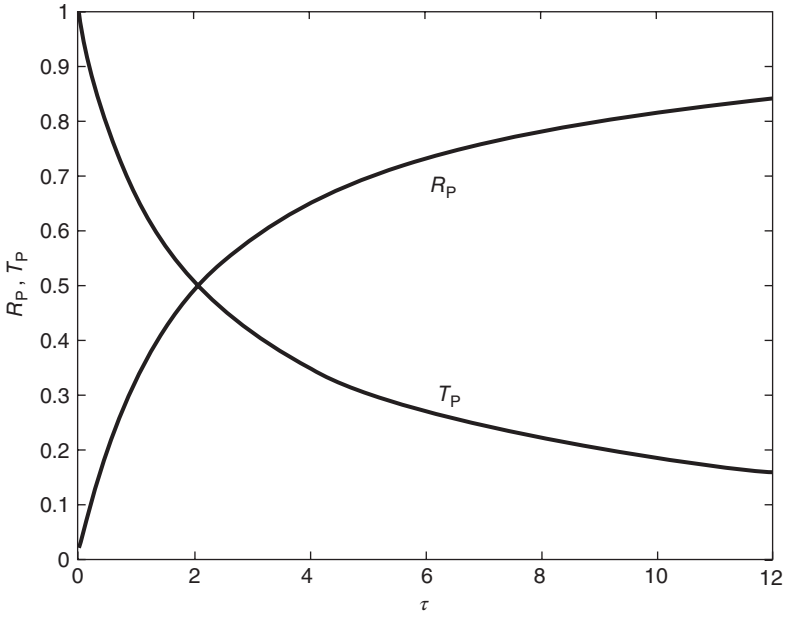

Figure 11 The reflectance and total transmittance as a function of γ_{tr} with $\gamma_a = 0$

Handbook of Digital Imaging, Online © 2015 John Wiley & Sons, Ltd.

This article was published in the *Handbook of Digital Imaging* in 2015 by John Wiley & Sons, Ltd.
DOI: 10.1002/9781118798706.hdi052

5 The Connection between PSF and Probability Approaches to Optical Dot Gain

It is possible to show a direct link, in accounting for optical dot gain, between the PSF approach and the probability approach [41–44]. As indicated earlier, in the probability approach, the probability of diffusion between different regions of the halftone microstructure is calculated, and these probabilities are used to account for optical dot gain. In this section, it is shown that the expression for the halftone reflectance is identical in the two cases, and that the probabilities can be calculated from the PSF.

One first derives a generalized Murray–Davis [26] model that takes into consideration optical dot gain. The reflectance is given by

$$\bar{R} = \mu \bar{R}_i(\mu) + (1 - \mu)\bar{R}_n(\mu), \tag{137}$$

where $\bar{R}$ is the average reflection from some region of the halftone, $\bar{R}_i$ is the reflectance from inked regions and $\bar{R}_n$ from noninked regions. The fractional area covered by ink is μ and $1 - \mu$ is the fractional area void of ink. One finds $\bar{R}_i$ and $\bar{R}_n$ by averaging $R(x, y)$ over the inked and noninked areas:

$$\bar{R}_i(\mu) = \frac{1}{\mu(Nr)^2} \int C(x, y)R(x, y)\mathrm{d}A \tag{138}$$

and

$$\bar{R}_n(\mu) = \frac{1}{(1 - \mu)(Nr)^2} \int [1 - C(x, y)]R(x, y)\mathrm{d}A \tag{139}$$

where $C(x, y)$ is 1 if the point (x, y) is inked and zero otherwise. Using Equation 10 for $R(x, y)$ and noting that $[C(x, y)]^2 = C(x, y)$ and that

$$\frac{1}{(Nr)^2} \int C(x, y)\mathrm{dA} = \mu, \tag{140}$$

and by Equations 21–24 that

$$\frac{1}{(Nr)^2} \int C(x, y)P(x, y)\mathrm{dA} = \mu^2 \mathcal{Z} \tag{141}$$

one finds

$$\bar{R}_i(\mu) = R_\mathrm{p} T_0[1 - (1 - T_0)\mu\mathcal{Z}] \tag{142}$$

and

$$\bar{R}_n(\mu) = R_\mathrm{p}\left[1 - (1 - T_0)\frac{\mu}{1 - \mu}(1 - \mu\mathcal{Z})\right]. \tag{143}$$

The connection between the PSF and probability approaches lies in the quantity $\mu\mathcal{Z}$.

In the following, the probability approach is outlined. One defines $P_\mathrm{I}(i)$ $[P_\mathrm{I}(n)]$ as the probability that a photon is incident in an inked region [noninked] region. Likewise, one defines $P_\mathrm{R}(i)$ $[P_\mathrm{R}(n)]$ as the probability that a photon is reflected from an inked [noninked] area. One further defines the conditional probability $P(i|i)$ $[P(i|n)]$ as the probability that if a photon entered

Handbook of Digital Imaging, Online © 2015 John Wiley & Sons, Ltd.

This article was published in the *Handbook of Digital Imaging* in 2015 by John Wiley & Sons, Ltd.
DOI: 10.1002/9781118798706.hdi052

the paper through an inked region it exits through an inked [noninked] region and finally one defines the conditional probability $P(n|i)$ $[P(n|n)]$ as the probability that if a photon entered the paper through a noninked area it exits through an inked [noninked] area. Further, T_0 can be interpreted as the probability that a photon is transmitted through the ink. Then, the following relations clearly hold:

$$P_{\mathrm{R}}(i) = P_{\mathrm{I}}(n)P(n|i)T_0 + P_{\mathrm{I}}(i)P(i|i)T_0^2 \tag{144}$$

$$P_{\mathrm{R}}(n) = P_{\mathrm{I}}(n)P(n|n) + P_{\mathrm{I}}(i)P(i|n)T_0. \tag{145}$$

For ease in notation one sets $R_{\mathrm{p}} = 1$. Clearly,

$$P_{\mathrm{I}}(i) = \mu \qquad P_{\mathrm{I}}(n) = 1 - \mu \tag{146}$$

and

$$P_{\mathrm{R}}(i) = \mu\bar{R}_i(\mu) \qquad P_{\mathrm{R}}(n) = (1 - \mu)\bar{R}_n(\mu). \tag{147}$$

The conditional probabilities are related in that

$$P(i|i) + P(i|n) = 1, \tag{148}$$

$$P(n|i) + P(n|n) = 1. \tag{149}$$

A detailed balance holds

$$P_{\mathrm{I}}(i)P(i|n) = P_{\mathrm{I}}(n)P(n|i), \tag{150}$$

which simply states that the probability of a photon entering an inked area and exiting a noninked area is the same as that of entering a noninked area and exiting an inked area. Defining $\beta \equiv P(i|i)$, one sees by Equation 148 that

$$P(i|n) = 1 - \beta, \tag{151}$$

and by Equation 149 and Equations 146 and 150

$$P(n|i) = \frac{\mu}{1 - \mu}(1 - \beta), \tag{152}$$

and by Equation 149

$$P(n|n) = 1 - \frac{\mu}{1 - \mu}(1 - \beta). \tag{153}$$

Substituting Equations 151 through 153 into Equations 144 and 145 using Equation 147, one finds

$$\bar{R}_i(\mu) = T_0[1 - (1 - T_0)\beta] \tag{154}$$

Handbook of Digital Imaging, Online © 2015 John Wiley & Sons, Ltd.

This article was published in the *Handbook of Digital Imaging* in 2015 by John Wiley & Sons, Ltd.
DOI: 10.1002/9781118798706.hdi052

and

$$\bar{R}_n(\mu) = \left[1 - (1 - T_0)\frac{\mu}{1-\mu}(1-\beta)\right]. \tag{155}$$

Comparing Equations 142 and 143 with Equations 154 and 155 shows that

$$\beta = \mu\mathcal{Z}.$$

One interprets $\mu\mathcal{Z}$ as $P(i|i)$, the conditional probability that if a photon enters though an inked area it will exit through an inked area. One can interpret $\mathcal{Z}^{-1}$ as a diffusion area –the area over which light diffuses: μ_{diff}. The ratio μ/μ_{diff} is the probability that a photon having entered the paper through a dot exits through a dot.

6 Summary

Optical dot gain has a significant effect on halftone tonality and is caused by photons diffusing within the paper. One of the ways that optical dot gain can be modeled is with a PSF. The halftone reflectance has been calculated using a PSF, and it is shown that effects of optical dot gain are contained within a single term – the Z-sum. $\mathcal{Z}$ is shown to be an effective diffusing area. A PSF has been derived in terms of the properties of the paper – the scattering and absorption coefficients – by solving the radiative transfer equation. Using the PSF, the average distance that photons diffuse within the paper has been calculated. An explicit expression for the Z-sum has been calculated, and it is shown that it can be approximated by the fractional ink coverage raised to a negative power between 0 and 1: $\mathcal{Z} \approx \mu^{-s}$, with $0 \leq s \leq 1$. The paper's reflectance and transmittance have been calculated. It is shown that there is a deep connection between the PSF approach and the probability approach to optical dot gain, in that $\mu\mathcal{Z}$ is identically the probability that a photon leaves the paper through a dot if it entered through a dot.

Appendix

In the following, a fast algorithm for calculating the eigenvalues and phases, μ_n and λ_n is derived. As $n \gg 1$, it follows that $\mu_n t \approx (n-1)pi$ and $\lambda_n \approx$ ß/2. One defines the quantity ε_n as

$$\mu_n t = (n-1)\pi + \varepsilon_n. \tag{156}$$

Then, for $n \gg 1$, $\varepsilon_n \approx 0$. As $\mu_n t = n\pi - 2\lambda_n$ (Equation 108), ε_n is related to λ_n by

$$\lambda_n = (\pi - \varepsilon_n)/2. \tag{157}$$

Using Equation 156 for μ_n in Equation 106, and taking the arctan of both sides one obtains

$$\varepsilon_n = \arctan\left[\frac{2\alpha\left\{(n-1)\pi + \varepsilon_n\right\}t^{=1}}{\alpha^2\{(n-1)\pi + \varepsilon_n\}^2 t^{-2} - 1}\right]. \tag{158}$$

Handbook of Digital Imaging, Online © 2015 John Wiley & Sons, Ltd.

This article was published in the *Handbook of Digital Imaging* in 2015 by John Wiley & Sons, Ltd.
DOI: 10.1002/9781118798706.hdi052

One chooses an initial value, such as π, for ε_n on the right-hand side, calculates the new ε_n, and iterates until it converges to a stable value:

$$\varepsilon_n^{(i)} = \arctan\left[\frac{2\alpha\left\{(n-1)\pi + \varepsilon_n^{(i-1)}\right\}t^{=1}}{\alpha^2\{(n-1)\pi + \varepsilon_n^{(i-1)}\}^2 t^{-2} - 1}\right].$$

Then, one uses Equations 156 and 157 to get μ_n and λ_n.

References

1. Yule, J. and Nielsen, W. (1957) The penetration of light into paper and its effect on halftone reproduction. *Technical Association of the Graphic Arts Proceedings*, **3**, 65–76.
2. Arney, J., Arney, C., and Engeldrum, P. (1996) Modeling the Yule–Nielsen effect. *Journal of Imaging Science and Technology*, **40**, 233–238.
3. Rogers, G. (1997) Optical dot gain in a halftone print. *Journal of Imaging Science and Technology*, **41**, 643–656.
4. Dainty, J. and Shaw, R. (1974) *Image Science*, Academic Press, London.
5. Engeldrum, P. (2004) Paper substrate spread function and the MTF of photographic paper. *Journal of Imaging Science and Technology*, **48**, 50–57.
6. Smith, J. (1995) Modulation transfer function for a CCD array with sample-and-hold operation on static waveforms. *Motion Imaging Journal*, **104**, 274–276.
7. Hu, J., Song, M., Sun, Y. *et al*. (1999) Measurement of modulation transfer function of charge-coupled devices using frequency-variable sine grating patterns. *Optical Engineering*, **38**, 1200.
8. Rogers, G. (1998) Measurement of the modulation transfer function of paper. *Applied Optics*, **37**, 7235–7240.
9. Yule, J., Howe, D., and Altman, J. (1967) The effect of the spread function of paper on halftone reproduction. *TAPPI Proceedings*, **50**, 337–344.
10. Engeldrum, P. and Pridham, B. (1995) Application of turbid medium theory to paper spread function measurements. *Technical Association of the Graphic Arts Proceedings*, pp. 339–354.
11. Wakeshima, H., Kunishi, T., and Kaneko, S. (1968) Light scattering in paper and its effect on halftone reproduction. *Journal of the Optical Society of America*, **58**, 272–273.
12. Ruckdeschel, F. and Hause, O. (1978) Yule-Nielsen effect in printing: a physical analysis. *Applied Optics*, **17**, 3376–3383.
13. Oittinen, P. (1982) Limits of microscopic print quality, in *Advances in Printing Science and Technology* (ed W.H. Banks), Pentech, London, pp. 121–128.
14. Arney, J., Arney, C., and Katsube, M. (1996) An MTF analysis of papers. *Journal of Imaging Science and Technology*, **40**, 19–25.
15. Arney, J., Pray, E., and Ito, K. (1999) Kubelka -Munk theory and the Yule-Nielsen effect on halftones. *Journal of Imaging Science and Technology*, **43**, 365–370.
16. Arney, J., Chauvin, J., Nauman, J. *et al*. (2003) Kubelka-Munk theory and the MTF of paper. *Journal of Imaging Science and Technology*, **47**, 339–345.
17. Yang, L. (2002) Modelling ink-jet printing -does the Kubelka-Munk theory apply? *NIP18: International Conference on Digital Printing Technologies*, San Diego, CA, pp. 482–485.
18. Yang, L. (2003) Ink-Paper interaction: a study in ink-jet color reproduction. Doctoral Dissertation, Linkoping University. NorrKoping, Sweden.
19. Yang, L. (2005) What has been overlooked in Kubelka Munk theory? *NIP21: International Conference on Digital Printing Technologies*, Baltimore, MD, pp. 376–379.
20. Yang, L. and Hersch, R. (2008) Kubelka-Munk Model for imperfectly diffuse light. *Journal of Imaging Science and Technology*, **52**, 1–7.
21. Mourad, S. (2003) Color predicting model for electrophotographic prints on common office paper. Disertation for Ecole Polytechnique Federale de Lausanne.
22. Mourad, S. (2007) Improved calibration of optical characteristics of paper by an adapted paper MTF model. *Journal of Imaging Science and Technology*, **51**, 283–292.

Handbook of Digital Imaging, Online © 2015 John Wiley & Sons, Ltd.

This article was published in the *Handbook of Digital Imaging* in 2015 by John Wiley & Sons, Ltd.
DOI: 10.1002/9781118798706.hdi052

23. For the case of penetrating ink see: Rogers, G. (2001) Penetrating ink and halftone reflectance. *Proceedings of the Society for Imaging Science and Technology PICS 2001 Conference*, Montreal, Quebec, pp. 59–63.
24. For the case of multiple internal reflections see: Rogers, G. (2000) A generalized Clapper Yule model of halftone reflectance. *Color Research and Application*, **25**, 402–407.
25. Sloane, N.J.A. (2010) The On Line Encyclopedia of Integer Sequences, published electronically at http://oeis.org, sequence A004018 (accessed 19 February 2014).
26. Arney, J., Engeldrum, P., and Zeng, H. (1995) An expanded murray-davies model of tone reproduction in halftone imaging. *Journal of Imaging Science and Technology*, **39**, 502–508.
27. Murray, A. (1936) Monochrome reproduction in photoengraving. *Journal of the Franklin Institute*, **221**, 721.
28. Case, K. and Zweifel, P. (1967) *Linear Transport Theory*, Addison Wesley, Reading, MA.
29. Chandrasekhar, S. (1960) *Radiative Transfer*, Dover Publications, New York.
30. Groenhuis, R., Ferwerda, H., and Bosch, J. (1983) Scattering and absorption of turbid materials determined from reflection measurements. 1: Theory. *Applied Optics*, **22**, 2456–2462.
31. Ishimaru, A. (1989) Diffusion of light in turbid material. *Applied Optics*, **28**, 2210–2215.
32. Ishimaru, A., Kuga, Y., Cheung, R. *et al*. (1983) Scattering and diffusion of a beam wave in randomly distributed scatterers. *Journal of the Optical Society of America*, **73**, 131–136.
33. Reynolds, L., Johnson, C., and Ishimaru, A. (1976) Diffuse reflectance from a finite blood medium: applications to the modeling of fiber optic catheters. *Applied Optics*, **15**, 2059–2067.
34. Haskell, R., Svaasand, L., Tsay, T. *et al*. (1994) Boundary conditions for the diffusion equation in radiative transfer. *Journal of the Optical Society of America A*, **11**, 2727–2741.
35. Bolt, R. and Ten Bosch, J. (1994) On the determination of optical parameters for turbid materials. *Waves in Random Media*, **4**, 233–242.
36. Scott, B., Abbott, J., and Trosset, S. (1995) *Properties of Paper*, TAPPI Press, Atlanta, GA.
37. Deng, M. and Dodson, C. (eds) (1994) *Paper: An Engineered Stocastic Structure*, TAPPI Press, Atlanta, GA.
38. Rance, H. (ed.) (1982) *Handbook of Paper Science*, Elsevier, New York.
39. Bristow, J. and Koldeth, P. (1986) *Paper: Structure and Properties*, Marcel Decker, New York.
40. Arfken, G. and Weber, H. (1995) *Mathematical Methods for Physicists*, 4th edn, Academic Press, New York.
41. Arney, J. (1997) A probability description of the Yule-Nielsen effect I. *Journal of Imaging Science and Technology*, **41**, 633–636.
42. Arney, J. and Katsube, M. (1997) A probability description of the Yule-Nielsen effect II: the impact of halftone geometry. *Journal of Imaging Science and Technology*, **41**, 637–642.
43. Rogers, G. (1998) Optical dot gain: lateral scattering probabilities. *Journal of Imaging Science and Technology*, **43**, 341–345.
44. Yang, L. (2014) The probability model for color tone reproduction, in *Handbook of Digital Imaging*, vol. 2, Chapter 29, John Wiley & Sons.

Handbook of Digital Imaging, Online © 2015 John Wiley & Sons, Ltd.

This article was published in the *Handbook of Digital Imaging* in 2015 by John Wiley & Sons, Ltd.
DOI: 10.1002/9781118798706.hdi052